

# Performance evaluation of the UV disinfection reactors by CFD and fluence simulations using a concept of disinfection efficiency

Huachen Pan and Marika Orava

## ABSTRACT

A CFD and UV fluence simulation program has been developed to evaluate the performance of drinking water disinfection reactors. Based on the flow field and the UV intensity field, the UV fluence or dose is obtained by solving the convection-diffusion partial differential equation of the fluence in the reactors. Eight UV-disinfection reactors from four manufacturers were evaluated. The fluence at the reactor outlet was evaluated using a logarithm microbial survival rate function. A calculated reduction equivalent fluence *CEF* was defined at the outlet and compared with the average fluence. That leads to a definition of a disinfection efficiency of the reactor. It is found that while the accurate prediction of the fluence level is difficult due to the difficulty in obtaining accurate lamp efficiency, quartz transmittance and reactor wall reflection rate etc., the accurate prediction of disinfection efficiency is quite possible because the uncertainties mentioned above have much less influence on efficiency prediction. The reactor's disinfection efficiency is mainly determined by the flow pattern, the lamp number and the lamp locations. These are primarily mechanical design issues for design optimization. Therefore the CFD and fluence modelling method presented in this paper can be useful for reactor design optimization.

**Key words** | CFD, disinfection, dose, efficiency, fluence, UV

**Huachen Pan** (corresponding author)  
Institute of Mechatronic Engineering,  
Hangzhou Dianzi University,  
310018, Hangzhou,  
China  
Tel.: +86-571-8152-6519  
Fax: +86-571-8603-2363  
E-mail: huachen\_pan@hdu.edu.cn

**Marika Orava**  
Ramboll Finland Oy,  
Laulukuja 6, 00420, Helsinki,  
Finland

## NOMENCLATURE

<i>A</i>	constant in logarithm microbial survival rate function
<i>B</i>	constant in logarithm microbial survival rate function
<i>CEF</i>	the calculated reduction equivalent fluence, J/m <sup>2</sup>
<i>REF</i>	the reduction equivalent fluence, J/m <sup>2</sup>
<i>F</i>	UV fluence, J/m <sup>2</sup>
<i>I</i>	UV radiation intensity or fluence rate, w/m <sup>2</sup>
<i>N</i>	number of survived microbes
<i>N</i> <sub>0</sub>	number of microbes before UV irradiation
<i>p</i>	pressure, N/m <sup>2</sup>
<i>Q</i>	flow rate, m <sup>3</sup> /h
<i>S</i>	a general source term

<i>SAK</i>	water spectral absorption coefficient
<i>u, v</i> and <i>w</i>	velocity components, m/s
<i>x, y</i> and <i>z</i>	Cartesian coordinates, m
<i>φ</i>	a general scalar quantity in a flow field
<i>η</i>	disinfection efficiency
<i>λ</i>	diffusion coefficient, m <sup>2</sup> /s
<i>μ</i>	viscosity, kg/m/s
<i>ρ</i>	density, kg/m <sup>3</sup>
<i>τ</i>	shear stress, N/m <sup>2</sup>

## INTRODUCTION

The UV disinfection reactors are used for many disinfection applications such as for drinking water, waste water, food

processing, etc. It is a device using UV radiation to disinfect the microbes in the fluid flowing through the reactor. To design a reactor with high disinfection performance and low energy consumption is the goal of the mechanical design optimization. Given the UV lamp properties, the key in the design is to arrange optimal lamp locations and flow patterns to make sure that the microbes in the fluid receive even exposure to the UV radiation. To achieve this, some quantitative performance indicators have to be defined such as device efficiency, to guide the design. The overall “efficiency” of a reactor is a matter of several factors such as the UV lamp efficiency, the spectrum of the lamps (the disinfection of microbes is spectrum-dependent), the transmittance of the fluid and the mechanical design of the reactor shape, which determines the flow pattern and radiation pattern. Some factors such as UV lamp efficiency and the spectrum of the lamp are factors that a reactor designer cannot control and optimize. However, with the available lamp types the mechanical designer can maximize the reactor performance, if the mechanism of disinfection is well understood.

CFD technology has been widely used to understand and predict the performance of UV disinfection devices. For example Janex *et al.* (1998) used CFD to optimize the reactor by modifying the geometry of the reactor aiming at reducing zones of low UV-dose or UV-fluence. Taghipour & Sozzi (2005) also found that the disinfection effect was strongly influenced by the reactor hydrodynamics in that a more uniform flow pattern and radiation distribution provided greater reactor performance under similar flow rate and UV lamp power. Sozzi & Taghipour (2006) and Unluturk *et al.* (2004) also intended to use CFD to accurately predict the UV fluence and compared with the biosimetric test. The attempt to accurately predict the UV radiation dose or UV fluence by CFD is difficult due to many factors. For example accurate information on lamp efficiency, which also changes with time as the lamps become old, is difficult to obtain. The radiation intensity prediction is also strongly influenced by the radiation model itself. For example Bolton (2000a) found that the reactor reflection can have more than 20% influence on the UV intensity level. Also the lamp quartz sleeve’s transmittance level may change when the reactor becomes dirty over time.

However, if the “electric efficiency” which tells how much of the electric energy turns into usable UV radiation energy is uncertain, then the “mechanical efficiency” on how much radiation energy turns into the disinfection effect is relatively certain using CFD predictions. In that sense, CFD may not be a very accurate tool in predicting the reactor fluence level, it however can be a powerful tool for the reactor’s mechanical design optimization.

Recently Elyasi & Taghipour (2006) suggested a definition of the reactor efficiency, which is defined by a calculated fluence divided by a theoretical maximum fluence. However the maximum fluence defined in (Elyasi & Taghipour 2006) is based on a volume weighted fluence rate and an average speed in the reactor. It is a rough estimation of the maximum fluence. Therefore the definition of the reactor efficiency itself may not be accurate.

In this study, we try to use a refined concept of reactor disinfection efficiency, based on a more reasonable definition on the average fluence a reactor can achieve at the reactor exit. We will give some CFD simulation examples to show the disinfection efficiency of several reactor products.

## THE CFD METHOD

A Navier-Stokes solver was used for flow modelling. The CFD code is a finite-volume, pressure-correction based solver, which uses multi-block structured grid to handle complicated geometries and multi-grid acceleration to ensure efficient solution on larger grids.

Turbulent viscosity is modelled by a standard k-ε model for core flow together with an algebraic turbulence model for boundary-layer flow. The near-wall treatment is carefully handled so that the skin friction accuracy is less dependent on the grid density near the wall.

For describing the steady viscous flow over a three-dimensional domain, we have the continuity equation

$$\frac{\partial}{\partial x}(\rho u) + \frac{\partial}{\partial y}(\rho v) + \frac{\partial}{\partial z}(\rho w) = 0 \quad (1)$$

and momentum equations

$$\begin{aligned} & \frac{\partial}{\partial x}(\rho uu) + \frac{\partial}{\partial y}(\rho vu) + \frac{\partial}{\partial z}(\rho wu) \\ &= -\frac{\partial p}{\partial x} + \frac{\partial}{\partial x}(\tau_{xx}) + \frac{\partial}{\partial y}(\tau_{yx}) + \frac{\partial}{\partial z}(\tau_{zx}) \end{aligned} \quad (2)$$

$$\begin{aligned} & \frac{\partial}{\partial x}(\rho uv) + \frac{\partial}{\partial y}(\rho vv) + \frac{\partial}{\partial z}(\rho vw) \\ &= -\frac{\partial p}{\partial y} + \frac{\partial}{\partial x}(\tau_{xy}) + \frac{\partial}{\partial y}(\tau_{yy}) + \frac{\partial}{\partial z}(\tau_{zy}) \end{aligned} \quad (3)$$

$$\begin{aligned} & \frac{\partial}{\partial x}(\rho uw) + \frac{\partial}{\partial y}(\rho vw) + \frac{\partial}{\partial z}(\rho ww) \\ &= -\frac{\partial p}{\partial z} + \frac{\partial}{\partial x}(\tau_{xz}) + \frac{\partial}{\partial y}(\tau_{yz}) + \frac{\partial}{\partial z}(\tau_{zz}) \end{aligned} \quad (4)$$

where  $x$ ,  $y$  and  $z$  are Cartesian co-ordinates,  $\rho$  density,  $u$ ,  $v$  and  $w$  velocities.  $p$  is pressure and  $\tau$  shear stress. For Newtonian fluids, under certain simplicity, we have

$$\begin{aligned} \tau_{xx} &= 2\mu \frac{\partial u}{\partial x} & \tau_{yy} &= 2\mu \frac{\partial v}{\partial y} & \tau_{zz} &= 2\mu \frac{\partial w}{\partial z} \\ \tau_{xy} &= \tau_{yx} = \mu \left( \frac{\partial v}{\partial x} + \frac{\partial u}{\partial y} \right) & \tau_{xz} &= \tau_{zx} = \mu \left( \frac{\partial w}{\partial x} + \frac{\partial u}{\partial z} \right) \\ \tau_{yz} &= \tau_{zy} = \mu \left( \frac{\partial v}{\partial z} + \frac{\partial w}{\partial y} \right) \end{aligned} \quad (5)$$

where  $\mu$  is viscosity. Further details of the flow solution method can be found from Pan (2000).

For the boundary conditions, velocity is given at all solid and inlet boundaries. At outlet boundary, velocities are extrapolated but with adjustment according to the inlet flow rate to meet mass flow balance requirement. The grid is extended far enough at outlet boundaries so that assumptions of the velocity distributions there have minimum effects on the flows in the areas of interest. The length of inlet pipe is seven times the diameter of the pipe, to obtain fully developed turbulent pipe flow.

## THE UV INTENSITY FIELD MODEL

The UV intensity calculation is based on the multiple point source summation (MPSS) method, which has been described by Bolton (2000a). The model takes quartz sleeve reflection and refraction into account. During the modelling

each lamp is divided into 100 sections and the UV intensity produced by each lamp piece is calculated in each grid cell.

Essential things in UV intensity modelling are light absorption in air, quartz and water. Wall shadowing is taken into account when path of light is calculated. In addition, reflection rate at reactor walls is also considered. Wide-band modelling for lamp power, germicidal effect and absorptions is used, when the performance of a medium pressure lamp reactor is studied.

## THE FLUENCE FIELD

The program solves fluence field using a convection-diffusion partial differential equation, of which the derivation is given in the Appendix:

$$\begin{aligned} \frac{\partial}{\partial x}(uF) + \frac{\partial}{\partial y}(vF) + \frac{\partial}{\partial z}(wF) &= \frac{\partial}{\partial x} \left( \lambda \frac{\partial F}{\partial x} \right) + \frac{\partial}{\partial y} \left( \lambda \frac{\partial F}{\partial y} \right) \\ &+ \frac{\partial}{\partial z} \left( \lambda \frac{\partial F}{\partial z} \right) + I(x, y, z) \end{aligned} \quad (6)$$

where  $F$  is fluence,  $u$ ,  $v$  and  $w$  are velocities,  $\lambda$  is diffusion coefficient (kinetic viscosity) and  $I$  is the local UV intensity.

After obtaining the UV intensity field  $I$  and flow field Equation (6) is solved to obtain a full 3-D fluence distribution:

$$F = F(x, y, z) \quad [\text{J/m}^2] \quad (7)$$

Since only the fluence at the outlet of the reactor is important, the fluence at a cross-section close to the intersection of the reactor and outlet pipe is collected and post processed. This is done to reduce distortion of results as a consequence of mixing phenomenon along the outlet pipe.

## FLUENCE VALUE HANDLING AT THE OUTLET OF THE REACTOR

To measure the mechanical efficiency of the reactor, the Calculated Reduction Equivalent Fluence (*CEF*) at a chosen outlet was defined (Orava 2003). The *CEF* is defined the same way as the Reduction Equivalent Fluence (*REF*) measured by biosimetry. The *CEF* calculation is based on

the microbial survival function shown in Equation (8), the fluence distribution at an outlet cross-section and the local flow rate distribution on the same cross-section.

The relation between fluence  $F$  and microbial survival rate  $N/N_0$  can be expressed as

$$F = -A \times \lg(N/N_0) + B \quad (8)$$

where  $A$  and  $B$  are constants.  $N$  is the number of microbes after irradiation and  $N_0$  is the number of microbes before irradiation.

Since at the outlet, the total microbial survival rate can be expressed as the flow-averaged value of the local microbial survival rate assuming  $N_0$  is equal at all cells at reactor inlet:

$$\left(\frac{N}{N_0}\right)_{total} = \frac{\sum 10^{-(F_{local}-B)/A} Q_{local}}{Q} \quad (9)$$

where  $(N/N_0)_{total}$  is the total survival rate of bacteria for a reactor,  $F_{local}$  is local fluence at a local calculation cell at the reactor outlet,  $Q_{local}$  is the flow at the local outlet cell face and  $Q$  is the total flow.

Then the  $CEF$  can be expressed as:

$$CEF = -A \times \lg((N/N_0)_{total}) + B \quad (10)$$

In addition to fluence distribution the model calculates minimum fluence  $F_{min}$ , maximum fluence  $F_{max}$ , and average

fluence  $F_{ave}$  in water exiting the reactor. The average fluence is calculated as the mass flow average across the outlet cross-section.

## DISINFECTION EFFICIENCY

At the reactor outlet, if the fluence distribution is absolutely even and has a constant value, then  $CEF$  equals to  $F_{ave}$ , we obtain the maximum efficiency of 100%. However for a practical reactor, the fluence at the outlet is not evenly distributed and  $CEF$  is always lower than  $F_{ave}$ . Therefore a parameter

$$\eta = CEF/F_{ave} \quad (11)$$

can be defined as the disinfection efficiency of the reactor. We call it disinfection efficiency because it is an indicator for the reactor to achieve the maximum utilization of the given UV radiation resources.

## SIMULATION EXAMPLES

Eight reactors from four manufacturers were evaluated. The reactors are presented in Table 1.

Calculation was done using two different flow rates and three SAK-values for each reactor. The SAK-value is the

**Table 1** | Reactors modelled in the project and the number of cells and nodes used in computational models

Reactor type	Lamp type	Nominal flow, m <sup>3</sup> /h	Number of cells	Number of nodes
A	Medium pressure	450	153 552	171 930
B	Medium pressure	150	130 824	145 103
C	Medium pressure	150	157 264	174 330
D	Medium pressure	700	184 296	204 551
E	Low pressure	400	301 600	333 232
F	Low pressure	150	184 912	204 738
G	Low pressure	150	170 640	207 936
H	Low pressure	80	147 240	170 867

water spectral absorption coefficient. SAK-1 means a water transmittance of 97.7% at 10 mm penetration length for the UV-C with wave length of 254 nm. SAK-3 means the water transmittance of 93.3% and SAK-5, 89.1%, respectively.

Flow rates may have varied more than the manufacturer suggested. Data of geometries and UV-C -power of lamps were collected from the manufacturers to obtain values as close to the manufacturer used values as possible in order to make the results more comparable with manufacturer table values.

The varying power of medium pressure lamps was taken into account by using the germicidal correction factor as defined by von Sonntag (Bolton 2000b). The lamp power was calculated at 5 nm intervals, which were multiplied with the appropriate germicidal correction factors. The wavelength-dependency of absorption of water was measured using nine samples from Finnish water utilities. The absorbance curves of surface water and ground water were used for modelling of medium pressure lamps. Also the absorbance of quartz glass varies, so the absorbance values were taken from (Bolton 2000a), except in one case where manufacturer values were used. Reflection from the reactor walls was studied from 0% to 30% and 10% was selected for the modelling, partly based on a study by Sommer *et al.* (1996).

An ideal microbe (survival curve coefficients  $A = 100$  and  $B = 0$ , Equation 10) was used to calculate the equivalent fluence. The survival curve coefficients of a real *Bacillus subtilis*-strain were used in one calculation to compare the difference between ideal and real bacteria. The difference in  $CEF$  was only 0,6% suggesting *B. subtilis* can be modelled using ideal microbe's survival curve coefficients around fluence  $400 \text{ J/m}^2$ . If higher or lower fluences are used, the difference may be greater.

## RESULTS AND DISCUSSION

To check the accuracy of the modelling, one computation was done using the same conditions such as the measured lamp power and water quality used in a biosimetric test. The test result was provided by the manufacturer. The survival curve of *Bacillus subtilis* was used. The reactor volume is about  $0.04 \text{ m}^3$ . The flow rate is  $400 \text{ m}^3/\text{s}$ . The calculated equivalent fluence of  $468 \text{ J/m}^2$  was only 5% higher than the biosimetric fluence. However, in most of the simulations, there are many

conditions, like lamp efficiency, quartz sleeve transmittance and reactor reflection rate etc. which cannot be accurately obtained. The  $CEF$  is highly dependent on those given conditions. Therefore an accurate prediction of the fluence level in general is difficult, if essential conditions like lamp efficiency etc. have to be guessed or assumed.

If we look at Equation (11), the uncertainty in the computational factors like the lamp power etc. have the same influence on  $CEF$  and on  $F_{ave}$  by increasing or decreasing their values by a factor. For example if we have an over-estimation of the lamp power by 20%, we may predict  $CEF$  and  $F_{ave}$  20% more than they should be. However, the disinfection efficiency  $\eta$  remains the same whether  $CEF$  and  $F_{ave}$  have increased by 20% or not. The disinfection efficiency is solely determined by the fluence unevenness in distribution at the outlet. Such uneven distribution is mainly caused by flow pattern and lamp locations, and therefore mainly determined by the mechanical design of the reactor. These “mechanical factors” like the flow pattern and the radiation pattern are highly predictable using the computational models. Therefore in this study we focus our attention on the disinfection efficiency only.

Figure 1 shows the disinfection efficiency for all eight products with different flow rates and water transmittances.

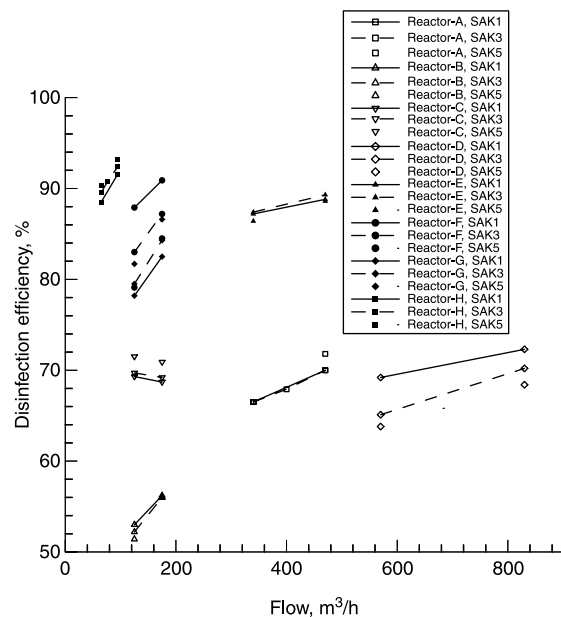
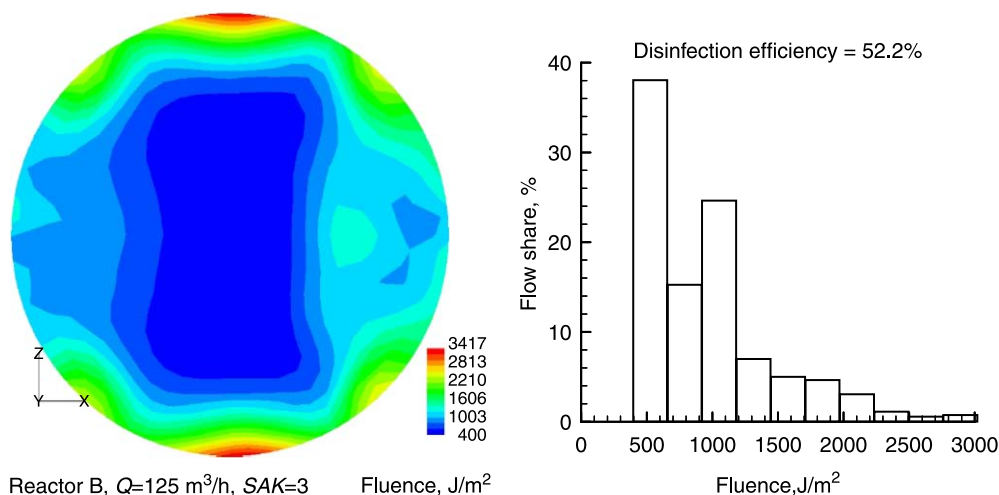


Figure 1 | Computed disinfection efficiencies of the eight reactors with different flow rates and water transmittances.



**Figure 2** | Fluence distribution at the outlet and the flow share of the fluence levels of the reactor B.

We can see that the individual designs have big differences in their disinfection efficiencies, ranging from around 50% to around 90%. It is interesting to notice that all reactors equipped with medium-pressure lamps (plotted using unfilled symbols) have lower efficiencies (from 51% to 73%) than those (from 79% to 93%) of the reactors equipped with low-pressure lamps (plotted using filled symbols). This is probably due to a larger amount of lamps in low-pressure-lamp reactors leading to smaller differences between luminous and dark areas.

The disinfection efficiency also changes when the flow rate changes or the water transmittance changes. However those changes are smaller compared with the differences among different reactors. The disinfection efficiency, with one exception, increases as the flow rate increases. The disinfection efficiency seems to have no clear correlation to the water transmittance, as indicated in Figure 1.

Among eight reactor products, 4 of them, the reactors B,C,F and G are for the same design flow rate  $150 \text{ m}^3/\text{h}$ . They have quite big difference in efficiency. Figures 2 to 5

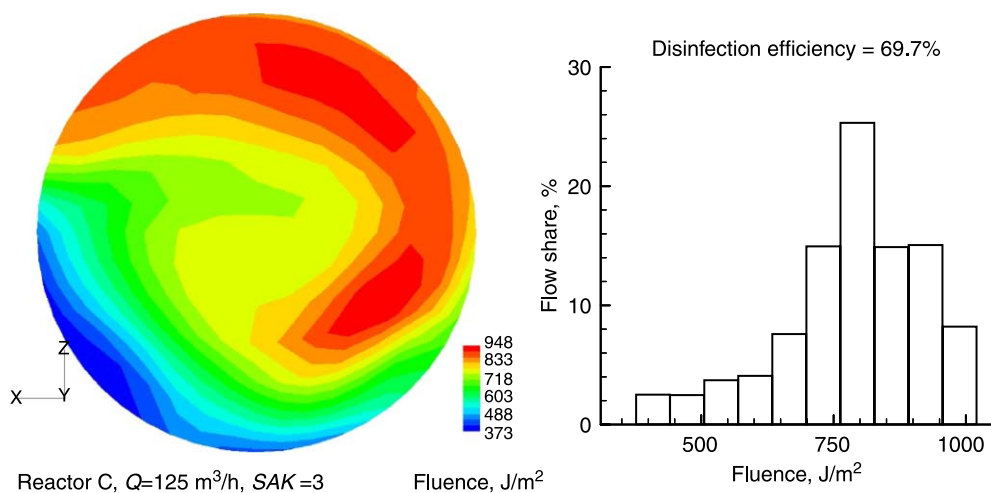


**Figure 3** | Fluence distribution at the outlet and the flow share of the fluence levels of the reactor C.

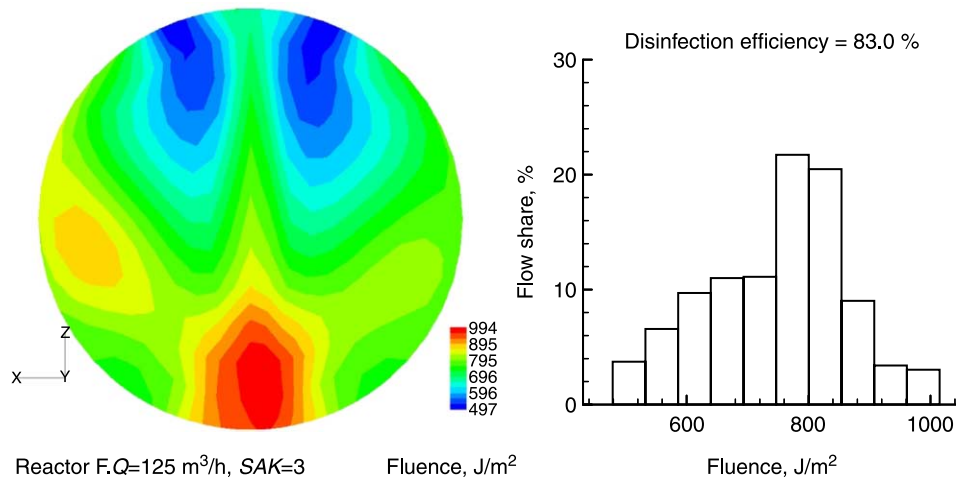


**Figure 4** | Fluence distribution at the outlet and the flow share of the fluence levels of the reactor F.

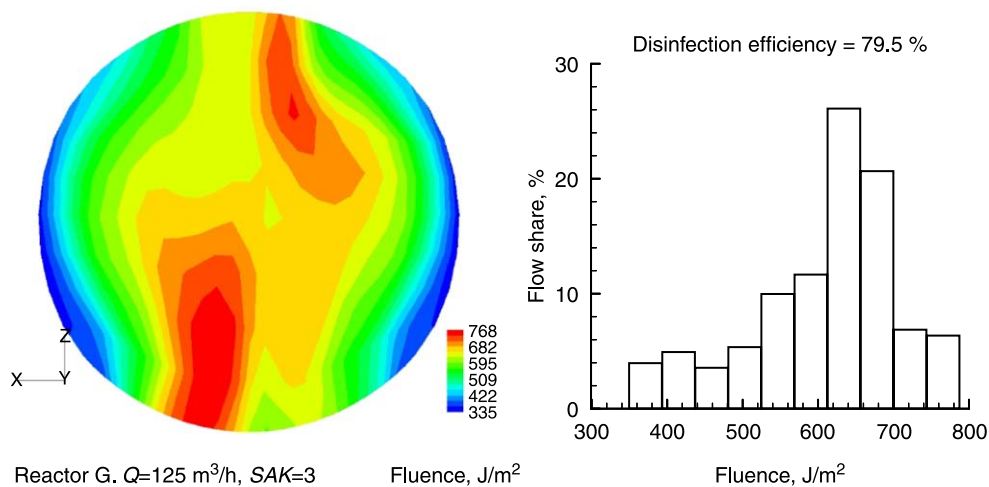


**Figure 5** | Fluence distribution at the outlet and the flow share of the fluence levels of the reactor G.

show these four reactors' outlet fluence distributions and the flow rate shares of their fluence levels using a water transmittance of SAK-3 and a flow rate of  $125 \text{ m}^3/\text{h}$ . Figure 2 shows the results of the reactor with the lowest efficiency. We can easily see that the reason for a low efficiency is an extremely uneven outlet fluence distribution, which produces a large flow share of the low fluence level. Reactors C, F and G, which have more even fluence distribution at the outlet and less flow shares of the low fluence level, have much higher efficiencies.

## CONCLUSIONS

CFD and fluence modelling is a useful tool to describe the physical phenomenon inside the UV disinfection reactors. The computational tool's accurate prediction on the fluence level may be difficult due to the difficulty in obtaining the accurate values of lamp efficiency, the quartz sleeve transmittance and the reactor wall reflection rate. However, those parameter uncertainties have much less influence on predicting the disinfection efficiency.

CFD and fluence simulations on eight reactors from four manufacturers show quite big differences in reactors' disinfection efficiencies among those reactors. The simulation results show that the unevenness of the fluence distribution at the reactor outlet is the reason for a low efficiency, especially when low fluence area in the reactor outlet has large flow share.

Whether the fluence has an even or uneven distribution on the outlet is highly determined by the flow pattern inside the reactor and by the lamp numbers and locations inside the reactor. Those factors are mainly a mechanical design issue, which can be optimized using the CFD and fluence modelling program.

The disinfection efficiency defined in this study is a useful concept for the manufacturers to optimize their reactors' design. The disinfection efficiency is also a useful concept for the reactor end users to select and dimension for their water supply system.

## ACKNOWLEDGEMENTS

The funding for the CFD and fluence modelling was provided by Ramboll Finland Oy. The funded work was mainly done at CFD-Finland Oy where the first author was working. Special thanks are given to Mr. Timo Laitinen whose vision made this work possible. We also thank Mr. Tapio Ala-Peijari for his many useful discussions.

## REFERENCES

- Bolton, J. 2000a Calculation of ultraviolet fluence rate distributions in an annular reactor: Significance of refraction and reflection. *Wat. Res.* **34**(13), 3315–3324.
- Bolton, J. 2000b Terms and definitions in ultraviolet disinfection, *Proc. of Disinfection 2000: Disinfection of Wastes in the New Millennium, March 15–18 2000, New Orleans, USA. Water Environment Federation, 601 Wythe st., Alexandria, VA, 22314-184, paper 1, Session 3.*
- Elyasi, S. & Taghipour, F. 2006 Simulation of UV photoreactor for water disinfection in Eulerian frame work. *Chemical Enging. Sci.* **61**(14), 4741–4749.
- Janex, M. L., Savoye, P., Do-Quang, Z., Blatchley, E. & Laine, J. M. 1998 Impact of water quality and reactor hydrodynamics on wastewater disinfection by UV, use of CFD modeling for performance optimisation. *Wat. Sci. Technol.* **38**(6), 71–78.
- Orava, M. 2003 *Ultraviolet Disinfection of Potable Water*. Tampere University of Technology, Department of Environmental Engineering. Masters Thesis (in Finnish), Tampere, Finland.
- Pan, H. 2000 Flow simulations for turbomachineries. In: *Proc. of 4th Asian Computational Fluid Dynamics Conference, Mianyang, China*, Zhang, H. (ed.), Univ. of Electronic Sci. and Tech. of China Press, Sichuan China, pp. 290–295.
- Sommer, R., Cabaj, A. & Haider, T. 1996 Microbicidal effect of reflected UV radiation in devices for water disinfection. *Wat. Sci. Technol.* **34**(7–8), 173–177.
- Sozzi, A. & Taghipour, F. 2006 UV reactor performance modelling by Eulerian and Lagrangian methods. *Env. Sci. Tech.* **40**(5), 1609–1615.
- Taghipour, F. & Sozzi, A. 2005 Medeling and design of ultraviolet reactors for disinfection by-product precursor removal. *Desalination* **176**(1–3), 71–80.
- Unluturk, S. K., Arastoopour, H. & Koutchma, T. 2004 Modeling of UV dose distribution in a thin-film UV reactor for processing of apple cider. *J. Food Enging.* **65**(1), 125–136.
- Versteeg, H. K. & Malalasekera, W. 1995 *An Introduction to Computational Fluid Dynamics*. Longman Scientific & Technical, Harlow, Essex, England.

## APPENDIX: DERIVATION OF THE EQUATION 6

If a microbe moves with the water flow along an infinitively short streamline  $ds$  for a time fraction  $dt$ , it receives the fraction of the UV disinfection fluence  $dF$  which can be expressed as

$$dF = I dt \quad (A1)$$

or

$$dF = I \frac{dt}{ds} ds \quad (A2)$$

or

$$dF = \frac{I}{\vec{V}} ds \quad (A3)$$

where  $\vec{V}$  is the velocity vector defined as

$$\vec{V} = \frac{ds}{dt} \quad (A4)$$

Obviously  $\frac{dF}{ds}$  is another vector, so (A3) can be expressed as

$$\vec{V} \bullet \frac{dF}{ds} = I \quad (A5)$$

or

$$u \frac{\partial}{\partial x}(F) + v \frac{\partial}{\partial y}(F) + w \frac{\partial}{\partial z}(F) = I \quad (\text{A6})$$

Introducing continuity equation, assuming density  $\rho$  is a constant, we have

$$\frac{\partial}{\partial x}(u) + \frac{\partial}{\partial y}(v) + \frac{\partial}{\partial z}(w) = 0 \quad (\text{A7})$$

Then Equation (A6) becomes

$$\frac{\partial}{\partial x}(uF) + \frac{\partial}{\partial y}(vF) + \frac{\partial}{\partial z}(wF) = I \quad (\text{A8})$$

From (A8) we see that the fluence is just like any other physical scalar quantity transported by the flow with a source term  $I$ . Up until this point, we have not considered any viscosity diffusion effect on this scalar quantity. To add viscous diffusive effect, we can examine the convection-diffusion equation of a general scalar in a viscous flow field. For a scalar  $\phi$  transported in a viscous flow, we have

(Versteeg & Malalasekera 1995):

$$\begin{aligned} \frac{\partial}{\partial x}(u\phi) + \frac{\partial}{\partial y}(v\phi) + \frac{\partial}{\partial z}(w\phi) &= \frac{\partial}{\partial x}\left(\lambda \frac{\partial \phi}{\partial x}\right) + \frac{\partial}{\partial y}\left(\lambda \frac{\partial \phi}{\partial y}\right) \\ &+ \frac{\partial}{\partial z}\left(\lambda \frac{\partial \phi}{\partial z}\right) + S(x, y, z) \end{aligned} \quad (\text{A9})$$

where  $\frac{\partial}{\partial x}(u\phi) + \frac{\partial}{\partial y}(v\phi) + \frac{\partial}{\partial z}(w\phi)$  are convection terms,  $\frac{\partial}{\partial x}\left(\lambda \frac{\partial \phi}{\partial x}\right) + \frac{\partial}{\partial y}\left(\lambda \frac{\partial \phi}{\partial y}\right) + \frac{\partial}{\partial z}\left(\lambda \frac{\partial \phi}{\partial z}\right)$  are diffusion terms and  $S(x, y, z)$  is a source term,  $\lambda$  is the diffusion coefficient, usually about the same value as the kinetic viscosity.

Comparing (A8) and (A9), if the fluence as a scalar quantity behaves the same way as any other scalars in the flow, we can add the diffusion terms used for any scalar in (A9). Then (A8) becomes:

$$\begin{aligned} \frac{\partial}{\partial x}(uF) + \frac{\partial}{\partial y}(vF) + \frac{\partial}{\partial z}(wF) &= \frac{\partial}{\partial x}\left(\lambda \frac{\partial F}{\partial x}\right) + \frac{\partial}{\partial y}\left(\lambda \frac{\partial F}{\partial y}\right) \\ &+ \frac{\partial}{\partial z}\left(\lambda \frac{\partial F}{\partial z}\right) + I(x, y, z) \end{aligned} \quad (\text{A10})$$

Here we assume that the diffusion coefficient is the same as kinetic viscosity. In turbulent flow it is the same as the effective turbulent kinetic viscosity, usually determined by a turbulence model in the practical computations.

First received 13 September 2006; accepted in revised form 11 December 2006